Energy & Environmental Science

Cite this: *Energy Environ. Sci.*, 2011, **4**, 4508

www.rsc.org/ees

COMMUNICATION

PVDF microbelts for harvesting energy from respiration†

Chengliang Sun,‡ Jian Shi, Dylan J. Bayerl and Xudong Wang*

Received 29th July 2011, Accepted 19th August 2011
DOI: 10.1039/c1ee02241e

In this paper, we report a technique that uses piezoelectric polyvinylidene fluoride (PVDF) microbelts to convert the energy from low-speed air flow to electricity *via* their resonant oscillation. The micrometre thick PVDF thin films were fabricated by a top-down reactive ion etching process, where the thickness was controlled by etching time and the piezoelectric phase was well preserved. The thickness, air flow speed and electrical output relationship was predicted theoretically and characterized experimentally. The PVDF microbelts were able to generate sufficient electrical energy from low speed air flow for the sustained operation of small electronic devices. Their capability for harvesting energy from simulated respiration was also demonstrated.

Harvesting energy from ambient mechanical energy sources has recently been shown to be a promising strategy for powering small electronics and eventually achieving self-powered electronic devices.[1–9] The self-powering capability allows electronic device packages to exclude bulky energy storage components and makes possible forgoing the inclusion of bulky battery components in an electronic device. The resultant small form factor is a particularly important feature for implantable biomedical devices. Recent development of nanogenerators has demonstrated a possible solution for the design of a self-sufficient implantable power source.[10–15] By using piezoelectric nanomaterials as the functional elements, low-density energies from heart beats, muscle stretching, or blood circulation may be converted into electricity *via* the direct piezoelectric effect.[16,17] The high structural quality and small dimensions of nanomaterials suggest that high energy conversion efficiency and sufficient output power are possible for nanogenerators with comparable size to that of the device itself. Compared to the above biological energy sources, respiration possesses the highest power capacity (~1 W) in the form of air flow.[18] Thus, scavenging energy from respiration would be promising for providing relatively high power to biomedical devices.

Several research efforts have been demonstrated to harvest energy from low-speed air flow at the device scale of centimetres and above. Most of them were based on the direct piezoelectric effect. Previous efforts to capitalize on low speed air flow as an energy source made use of piezoelectric cantilever beams,[19,20] windmills,[21] and inductive wind belt Windbelt™. The cut-in wind speed (minimum wind speed needed to drive the oscillation) of these designs was typically ~2 m s^{-1} and above. Considering the fluctuating air flow speed during normal breath (typically from 0 to ~2 m s^{-1}),[22] harvesting this energy requires a device of smaller size and lower cut-in wind speed than previously achieved. In addition, a flexible material with high toughness is desired for avoiding fatigue failure under long-term continuous oscillation during operation.

β-Phase PVDF has piezoelectric coefficients of ~−20 to 30 (d_{33}) and ~18 (d_{31}) pC/N,[23] sufficient to generate appreciable voltage under strain. Its room-temperature mechanical property allows it to be used where high strains or large deflections are always experienced.

Department of Materials Science and Engineering, University of Wisconsin—Madison, Madison, WI, 53706, USA. E-mail: xudong@engr.wisc.edu; Fax: +1 608-2628353; Tel: +1 608-8902667

† Electronic supplementary information (ESI) available: Simulation of vibration, calculation of voltage and power output, and video of powering a stopwatch. See DOI: 10.1039/c1ee02241e

‡ Current address: Institute of Microelectronics, Singapore Science Park II, Singapore 117685.

Broader context

A long-lifetime power supply is greatly desired for implantable biomedical devices, which can reduce the time of surgery that may be needed for replacing batteries. One promising solution is to directly harvest energy from the surroundings, *i.e.* from the biological system itself, thus to realize self-powered biomedical devices. This capability requires the energy-harvesting devices having comparably small sizes, good biocompatibility, as well as specific designs that can respond well to different bio-energy sources. The recently developed piezoelectric nanowire-based nanogenerators have been recognized as a promising concept for nanoscale mechanical energy scavenging, which is particularly useful for implantable biomedical devices. The energy sources that can be harvested by current nanogenerator designs are mostly based on acoustic waves or external force fluctuations. The research presented in this paper is a significant progress leading toward a practical micro-scale device for harvesting energy from a regular human activity—respiration. The energy harvesting relies on the oscillation of PVDF microbelts, whose geometry allows resonant oscillation to be excited by low-speed air flow. This capability has the potential for powering implantable biomedical devices.

A number of devices for mechanical energy harvesting have been demonstrated using PVDF films or nanostructures.[24–28] Its good biocompatibility allows PVDF to be used in a biological system for energy harvesting.[28,29] In order to design a PVDF belt that can produce resonant oscillation under low-speed air flow, the thickness of the PVDF belt needs to be small. However, formation of piezoelectric β-phase PVDF requires application of large tensile strain, which fundamentally limits the minimum thickness of a β-phase PVDF thin film because a certain level of mechanical strength is required to survive the β-phase formation by stretching without rupture.[30] Thus, there exists a minimum β-phase film thickness which can be produced *via* this method. Although doping[31,32] and copolymerization[33] were applied to make piezoelectric PVDF thin films with thicknesses in the nanometre regime, these approaches jeopardize the mechanical toughness of the thin films. In this paper, we report a reactive ion etching (RIE) technique for thinning commercial β-phase PVDF thin films. The β-phase was well-preserved after the thickness was reduced from 26 to 11 microns. The film thickness-related air-flow energy conversion capability was characterized. We demonstrated that such a thin film could provide sufficient power for sustaining regular operation of a small electronic device.

β-Phase PVDF films were received from Measurement Specialties Inc. and the original film thickness was measured to be 26 μm. The as-received β-phase PVDF films were processed by RIE (Plasma-Therm 790, 250 W operation power) to reduce the thickness. The sample was placed in the chamber with a tilting angle of ~15 degrees away from the horizontal surface. The pressure of the etching chamber was held at 50 mTorr with a constant reactive gas flow including 2 sccm of CF_4 and 80 sccm of O_2. The etching process was stopped for 10 minutes after every 5 minute operation to avoid high temperature damage to the sample.

Thicknesses of RIE-treated PVDF films were measured by a profilometer with a resolution of 5 nm and plotted as a function of time (Fig. 1a). A linear relationship can be clearly observed, which suggests an etching rate of ~0.41 μm min^{-1}. The top inset of Fig. 1a shows a typical topography of the etched PVDF surface. AFM characterization revealed that the average surface roughness tended to decrease from ~600 nm after 15 minute etching to ~500 nm after longer etching processes. As shown in the bottom inset of Fig. 1a, the roughness appeared to have little dependence on the etching time, which may be attributed to non-perpendicular ion beam incidence resulting in significant interaction volume overlap of ions on the polymer surface.[34] This observation implies that control of surface roughness could be further improved by adjusting the incident angle of the ion beam or optimizing the etching parameters.

The phase of processed PVDF films was confirmed by FTIR spectra. As shown in Fig. 1b, identical IR absorption peaks were obtained from the 6 samples with different etching times including as-received (red curve). The characteristic peaks of β-phase PVDF at 1275 and 840 cm^{-1} can be clearly distinguished in all samples.[35] This result shows that the thickness of PVDF films can be tuned down to micrometre levels by RIE with its piezoelectric β-phase unaffected. The film thickness could be potentially tuned to the sub-micrometre level given improved surface smoothness. Therefore, this technique successfully circumvented the challenging α- to β-phase conversion step after reaching the desired thickness, and thus is promising for fabricating free-standing piezoelectric PVDF thin films with controlled thickness.

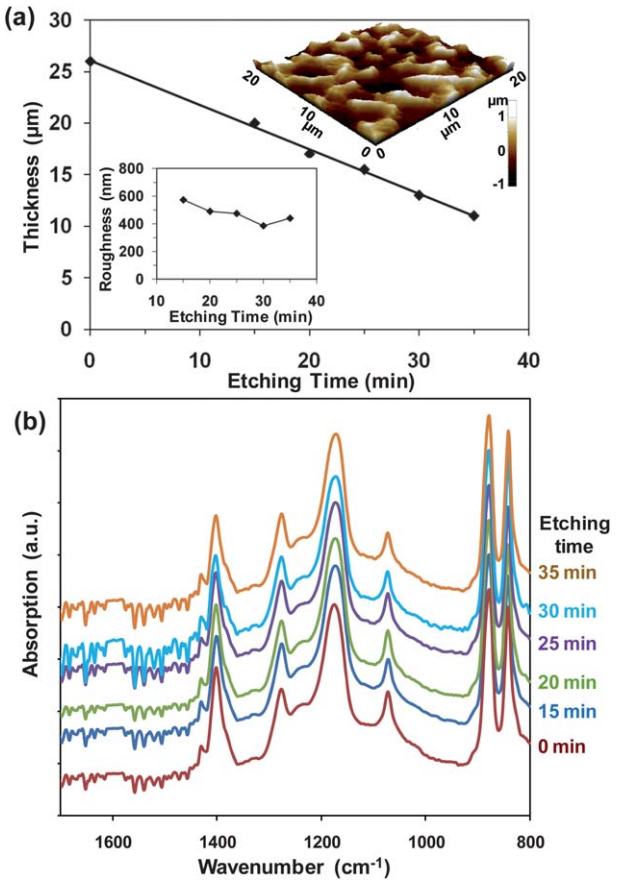

Fig. 1 RIE processing of PVDF thin films. (a) Plot of PVDF film thickness *versus* etching time. Top inset: AFM image showing the topography of the as-etching PVDF surface. Bottom inset: surface roughness *versus* etching time. (b) FTIR spectra of PVDF thin films processed by RIE for different times.

To make an energy harvesting device, a layer of Au was deposited on both sides of the PVDF thin films as electrodes. The film was then poled under an electric field of 70 MV m^{-1} for 5 minutes and cut into 20 mm × 2 mm belts with the length direction parallel to the β-phase forming tensile direction. The design for characterizing the capability of harvesting energy from air flow is schematically shown in Fig. 2a. The PVDF microbelt (MB) was tightly suspended across the front edge of a trench which was ~1 cm deep. The air flow was provided by a nozzle placed ~3 cm in front of the trench and the flow speed was measured at the position where the MB was located. Direct measurement of the voltage difference between the top and bottom electrodes of the PVDF MB demonstrated that the appreciable piezoelectric potential was produced by low-speed air flow. Fig. 2b shows the open-circuit voltage (V_{OC}) of a 26 μm thick PVDF MB as a function of air flow speed. Peak V_{OC} of ~±6 V was detected at an air flow speed of 5 m s^{-1} (the maximum speed tested). The voltage amplitude monotonically decreased following the reduction of air flow speed. At the air flow speed of ~1 m s^{-1}, the output voltage dropped to less than 0.1 V due to the very small oscillation amplitude (inset of Fig. 2b).

Theoretically, a bridging belt of suspended length L, such as in Fig. 2a, can be driven into resonant oscillation (galloping) under laminar fluid flow when its structural and dynamical properties

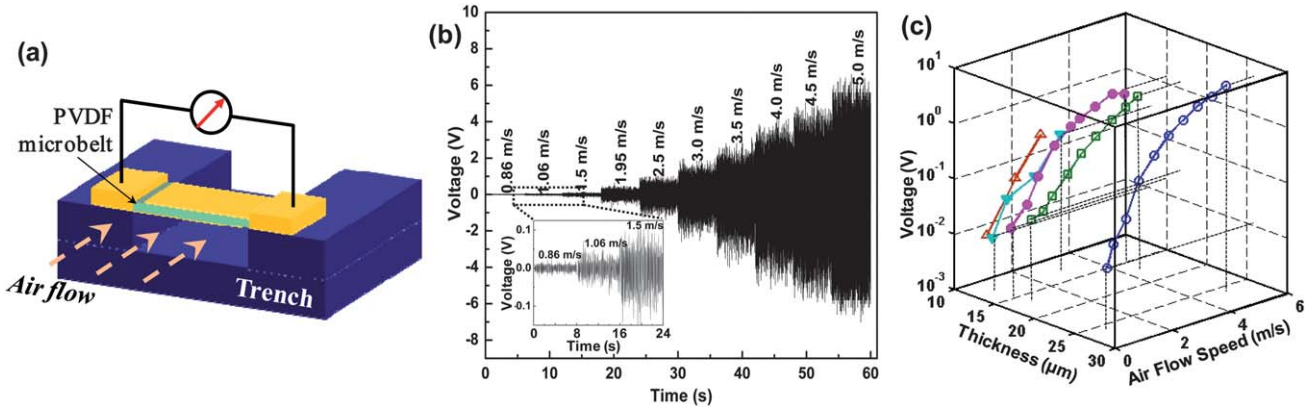

Fig. 2 (a) Schematic design of a PVDF microbelt for harvesting energy from air flow. (b) Open-circuit voltage measured under different air flow speeds. (c) 3D plot of the measured open-circuit voltage output as functions of the PVDF film thickness and air flow speed.

satisfy the critical conditions (see ESI S1† for details).[36] Calculations for the PVDF belt showed that it can be driven into resonant oscillation at an air flow speed as low as ~1 m s^{-1} (see ESI S1†), where the effect of the Au electrodes was neglected. Based on this relationship and the piezoelectric properties of PVDF, a numerical calculation was performed to predict the output voltage as a function of the air flow speed and thickness of PVDF MBs (see ESI S2 and Fig. S3†). The 0 V region means MBs with those dimensions cannot be driven into resonant oscillation by that air flow speed. For example, for a 26 μm thick MB (the dimension used to generate Fig. 2b), the air flow speed has to be higher than ~0.6 m s^{-1} in order to induce the resonant oscillation. This result is close to our experimental observation. As demonstrated in the inset of Fig. 2b, although very small (~0.01 V), a continuous voltage signal was produced at an air flow speed of 0.86 m s^{-1}, indicating an oscillation of the PVDF MB. However, the measured V_{OC} was still 1–2 orders of magnitude smaller than the calculated values. Such big discrepancies are possibly due to incomplete poling of our PVDF films and the large surface roughness that could lead to lower capacitance and reduced oscillation amplitudes.

In general, reducing the belt thickness could lower the cut-in speed of air flow as well as improve the voltage output at the same air flow speed provided the maximum strain is not reached. PVDF MBs with a series of thickness from ~10 μm to 26 μm were tested to investigate their capability of converting low-speed air flow energy into electricity. Appreciable V_{OC} was detected from PVDF MBs of all thickness tested further proving that the etching technique could preserve piezoelectric properties whilst effectively reducing the PVDF film thickness. At relatively high air flow speed (>3 m s^{-1}), thicker belts (>15 μm) produced stable voltage output from hundreds of mV to a few volts. The thinner belts (~10 and 13 μm) were unable to operate at air flow speeds higher than 3 m s^{-1}, which would have damaged the MBs from the large strain generated. At relatively low air flow speed (<2 m s^{-1}), thinner PVDF films exhibited higher voltage output compared to thicker films. At an air flow speed of ~1.5 m s^{-1}, 15 μm thick MB yielded ±123 mV voltage output; while the output from the original PVDF MB (26 μm) was only ±75 mV. All the MBs with thickness from ~13 to 17 μm exhibited >10 mV voltage output under an air flow speed of ~0.5 m s^{-1} (the lowest flow speed quantifiable by our equipment). Under the same air flow speed, no output could be detected from the original PVDF MB since its oscillation could not be excited by such a low flow speed. However, the ~10 μm thick MB was not able to produce the expected higher voltage output. This is possibly due to the large surface roughness and Au electrode layers mitigating its oscillatory behavior. We believe this limitation could be overcome by optimizing the etching recipe to improve the smoothness of surface and/or selecting electrodes with negligible weight and volume, such as graphene.

Based on the output voltage prediction, corresponding electric power was estimated *via* the relation

$$P = V_{RMS}^2/4R \quad (1)$$

where V_{RMS} is the root mean square of the oscillating voltage output, and R is the matching load for extracting the highest possible power. For the PVDF MBs that were used in our experiments, the resistivity ρ was experimentally determined to be ~1.2 × 10^5 Ωm. Thus the matching load was determined for PVDF MBs with different thicknesses ($R = \rho H/A$, H is the film thickness and A is the electrode area). The prediction of output power as functions of the air flow speed and film thickness is included in the ESI (Fig. S4†). The analysis suggests that thinner films are able to produce higher output power under low-speed air flow (<1 m s^{-1}).

Using the same series of PVDF MBs, the thickness-related power output was experimentally determined. A variable resistor was connected to the MBs for measuring the V_{RMS} at different load resistances. The output power was calculated for each load value *via* eqn (1), from which the maximum output power was obtained and the corresponding resistance could be considered as the optimal matching load (Fig. S5†). Through this method, the maximum possible output power of each MB was determined as a function of air flow speed and plotted in Fig. 3a. A similar power–thickness–air flow speed relationship was obtained as the open circuit voltage shown in Fig. 2c. The output power in the range of nW–μW can be produced by PVDF MBs in an air flow speed lower than 1 m s^{-1}. Integrating more PVDF MBs together could further improve the output power but a rectifying circuit is needed for each MB.

By connecting the PVDF MB to a capacitor (1 mF) through a bridge circuit, a practical direct current (DC) power source was demonstrated. The equivalent circuit is schematically shown in the inset of Fig. 3b. The charging process of the capacitor during MB oscillation was monitored by measuring the voltage on the capacitor.

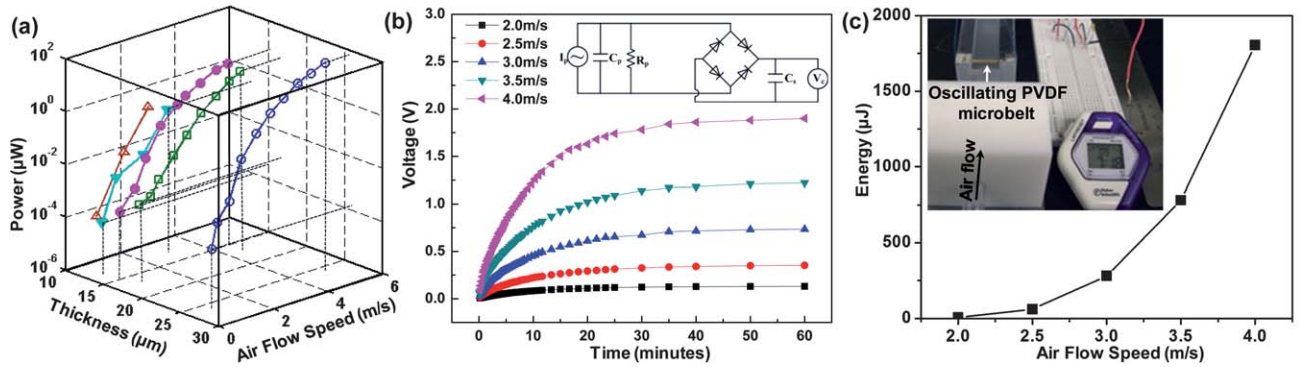

Fig. 3 Power output from PVDF MBs. (a) 3D plot of the deduced maximum power output as functions of the PVDF film thickness and air flow speed. (b) Measured voltage on a capacitor charged by a PVDF MB under different wind speeds. The inset shows the equivalent circuit. (c) Energy stored by the capacitor under different wind speeds. The inset shows an operating stopwatch powered by one MB under an air flow speed of ~3.5 m s^{-1}.

The 20 minute etched PVDF MB (~17 μm thick) was used in this system. The bridge circuit increased the cut-in air flow speed to ~1.5 m s^{-1} for this PVDF MB due to the diode turn-on voltage. As shown in Fig. 3b, higher air flow speed produced faster charging rate on the capacitor. The voltage eventually reached a saturation point due to the equilibrium established between the charging rate and the capacitor leakage rate. Based on the saturation voltage that can be eventually maintained on the capacitor under different air flow speeds, the usable energy stored in the capacitor from MB oscillation was determined as a function of the air flow speed (Fig. 3c). The maximum stored energy increased from ~8 μJ at 2 m s^{-1} to 1.8 mJ at 4 m s^{-1}. This energy level is sufficient to power small electronic devices, which was demonstrated using a digital stopwatch. As shown in the inset of Fig. 3b, the stopwatch was connected as a load on the capacitor. By applying constant air flow at a speed of 3.5 m s^{-1}, the stopwatch was operated normally (see the video in the ESI†). Sustained production of useful levels of electrical power by PVDF MBs under low-speed air flow was thus demonstrated.

The small size of PVDF MBs and their capability of producing μW level power under low-speed air flow make feasible harnessing energy from respiratory processes. The air flow rate of normal adult human respiration follows a sine curve with a peak rate of ~0.4 l s^{-1} (corresponding to ~2 m s^{-1} considering the average area of adult human nostrils) and a periodicity of ~5 to 6 s.[22] Respiration during exercise could increase the air flow rate by 4–8 times suggesting a higher energy capacity. Here we only consider the air flow of normal respiration. Certainly, the lower cut-in speed would allow more energy to be harvested by a MB. Since the 17 μm thick PVDF belt exhibited the best performance under air flow <2 m s^{-1}, it was selected for device fabrication. Such a belt was fixed at the center of a cylindrical channel with a cross-sectional area of ~1 cm^2. One end of the channel was connected to a compressible plastic chamber that simulated the function of a lung and the other end was open (Fig. 4a). The plastic chamber was squeezed and released every 6 seconds producing air flow in and out through the tunnel with a peak rate of ~2.3 m s^{-1} (Fig. 4b, calculated from the volume change of the plastic chamber per unit time of ~0.23 l s^{-1}). This operation provided a close simulation of typical adult's respiration.

Resonant oscillation of the MB was stimulated by the air flow through the channel and its V_{OC} output was continuously monitored. The voltage output was clearly correlated to the instantaneous flow

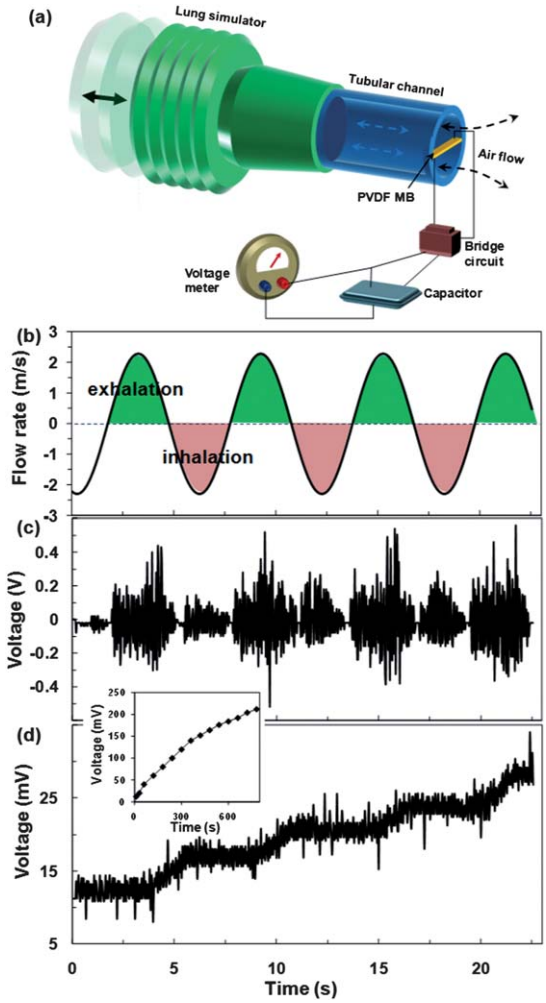

Fig. 4 Energy harvesting from simulated respiration by PVDF MBs. (a) Schematic design for simulated respiration energy harvesting. (b) Air flow rate through a tubular channel with a matching pattern to the normal respiration of an adult. (c) Corresponding V_{OC} measured on a PVDF MB fixed at one end of the tubular channel. (d) Voltage increase on a capacitor that was connected to the PVDF MB through a bridge circuit. The inset shows the long-term voltage increase trend on the capacitor.

rate and peak voltage output of ~0.4 to 0.5 V was detected at the highest "exhalation" flow rate of ~0.5 l s^{-1} (Fig. 4c). Lower output voltage was observed during "inhalation" cycles. This was likely due to the asymmetry of the air flow profile between inhalation and exhalation. In order to demonstrate the feasibility of converting energy from respiration to useful electricity, a 1 mF capacitor was connected to the MB through a bridge circuit and the increasing voltage curve is shown in Fig. 4d. It reveals that one respiration cycle could increase the capacitor voltage by ~5 mV. A majority of the voltage increase was registered with the "exhalation" cycles owing to the higher voltage output of the MB. A continuous 12 minutes of simulated respiration produced a capacitor voltage output of ~200 mV, corresponding to 20 μJ of electrical energy storage.

In conclusion, we demonstrated a top-down RIE approach to fabricate micrometre thick piezoelectric PVDF thin films from commercial β-phase PVDF thick films. The film thickness was controlled by etching time and the β-phase was well preserved during etching. This technique circumvented the challenging α- to β-phase conversion step for making free-standing piezoelectric PVDF thin films. With measures to improve surface smoothness, we expect the thickness could be controlled down to a submicron level. MB structures made from the PVDF thin films were shown to oscillate under low-speed air flow and generate electrical energy sufficient for powering small electronic devices. This capability is ideal for harvesting energy from respiration, and thus has the potential for powering implantable biomedical devices.

Acknowledgements

We thank Dr Shengguo Lu for helpful discussion and the comments from Mr M. Starr. We also thank the support of National Science Foundation under grant no. DMR-0905914, the UW-Madison graduate school and DARPA under grant No. N66001-11-1-4139.

Notes and references

1 J. A. Paradiso and T. Starner, *IEEE Pervasive Comput.*, 2005, **4**, 18–27.
2 J. M. Donelan, Q. Li, V. Naing, J. A. Hoffer, D. J. Weber and A. D. Kuo, *Science*, 2008, **319**, 807–810.
3 G. K. Ottman, H. F. Hofmann, A. C. Bhatt and G. A. Lesieutre, *IEEE Trans. Power Electron.*, 2002, **17**, 669–676.
4 S. Priya, *J. Electroceram.*, 2007, **19**, 167–184.
5 A. P. Chandrakasan, N. Verma and D. C. Daly, *Annu. Rev. Biomed. Eng.*, 2008, **10**, 247–274.
6 G. Poulin, E. Sarraute and F. Costa, *Sens. Actuators, A*, 2004, **116**, 461–471.
7 R. S. Yang, Y. Qin, L. M. Dai and Z. L. Wang, *Nat. Nanotechnol.*, 2009, **4**, 34–39.
8 S. Xu, Y. Qin, C. Xu, Y. Wei, R. Yang and Z. L. Wang, *Nat. Nanotechnol.*, 2010, **5**, 366–373.
9 M. Lee, J. Bae, J. Lee, C.-S. Lee, S. Hong and Z. L. Wang, *Energy Environ. Sci.*, 2011, **4**, 3359–3363, Advance article.
10 R. F. Service, *Science*, 2010, **328**, 304–305.
11 X. D. Wang, J. H. Song, J. Liu and Z. L. Wang, *Science*, 2007, **316**, 102–105.
12 C. Chang, V. H. Tran, J. Wang, Y.-K. Fuh and L. Lin, *Nano Lett.*, 2010, **10**, 726–731.
13 Z. L. Wang, X. D. Wang, J. H. Song, J. Liu and Y. F. Gao, *IEEE Pervasive Computing*, 2008, **7**, 49–55.
14 Y. Qin, X. D. Wang and Z. L. Wang, *Nature*, 2008, **451**, 809–813.
15 X. Chen, S. Xu, N. Yao and Y. Shi, *Nano Lett.*, 2010, **10**, 2133–2137.
16 Z. L. Wang, *Sci. Am.*, 2008, **298**, 82–87.
17 Y. Qi and M. C. McAlpine, *Energy Environ. Sci.*, 2010, **3**, 1275–1285.
18 T. Starner, *IBM Syst. J.*, 1996, **35**, 618–629.
19 D. St. Clair, A. Bibo, V. R. Sennakesavababu, M. F. Daqaq and G. Li, *Appl. Phys. Lett.*, 2010, **96**, 144103.
20 J. Ji, F. Kong, L. He, Q. Guan and Z. Feng, *Jpn. J. Appl. Phys.*, 2010, **49**, 050204.
21 S. Priya, C. T. Chen, D. Fye and J. Zahnd, *Jpn. J. Appl. Phys.*, 2005, **44**, L104–L107.
22 J. K. Gupta, C.-H. Lin and Q. Chen, *Indoor Air*, 2010, **20**, 31–39.
23 P. Ueberschlag, *Sens. Rev.*, 2001, **21**, 118–125.
24 N. S. Shenck and J. A. Paradiso, *IEEE Micro*, 2001, **21**, 30–42.
25 L. Mateu and F. Moll, *J. Intell. Mater. Syst. Struct.*, 2005, **16**, 835–845.
26 J. Kymissis, C. Kendall, J. Paradiso and N. Gershenfeld, *Second International Symposium on Wearable Computers*, 1998, pp. 132–139.
27 G. Jonathan, J. Feenstra, H. A. Sodano and K. Farinholt, *Smart Mater. Struct.*, 2007, **16**, 1810.
28 B. J. Hansen, Y. Liu, R. Yang and Z. L. Wang, *ACS Nano*, 2010, **4**, 3647–3652.
29 G. Laroche, Y. Marois, R. Guidoin, M. W. King, L. Martin, T. How and Y. Douville, *J. Biomed. Mater. Res.*, 1995, **29**, 1525–1536.
30 P. Calvert, *Nature*, 1975, **256**, 694.
31 X. He and K. Yao, *Appl. Phys. Lett.*, 2006, **89**, 112909.
32 X. Li, S. Chen, K. Yao and F. E. H. Tay, *J. Polym. Sci., Part B: Polym. Phys.*, 2009, **47**, 2410–2418.
33 Q. M. Zhang, V. Bharti and X. Zhao, *Science*, 1998, **280**, 2101–2104.
34 J. R. Morber, X. D. Wang, J. Liu, R. L. Snyder and Z. L. Wang, *Adv. Mater.*, 2009, **21**, 2072–2076.
35 Y. Bormashenko, R. Pogreb, O. Stanevsky and E. Bormashenko, *Polym. Test.*, 2004, **23**, 791–796.
36 R. D. Blevins, *Flow-Induced Vibration*, Van Nostrand Reinhold, New York, 1990.

